RSC Advances

PAPER

View Article Online
View Journal | View Issue

Cite this: *RSC Adv.*, 2020, **10**, 41901

Synthesis and evaluation of (*S*)-5′-*C*-aminopropyl and (*S*)-5′-*C*-aminopropyl-2′-arabinofluoro modified DNA oligomers for novel RNase H-dependent antisense oligonucleotides†

Yujun Zhou,[a] Ryohei Kajino,[a] Seiichiro Ishii,[e] Kenji Yamagishi[e] and Yoshihito Ueno *[abcd]

Received 5th October 2020
Accepted 10th November 2020

DOI: 10.1039/d0ra08468a

rsc.li/rsc-advances

We designed and synthesized two novel thymidine analogs: (*S*)-5′-*C*-aminopropyl-thymidine and (*S*)-5′-*C*-aminopropyl-2′-β-fluoro-thymidine. Then, DNA oligomers containing these analogs were synthesized, and their functional properties were evaluated. Compared with the naturally occurring thymidine, it was revealed that (*S*)-5′-*C*-aminopropyl-2′-arabinofluoro-thymidine was sufficiently thermally stable, while (*S*)-5′-*C*-aminopropyl-thymidine featured thermal destabilization. The difference in thermal stability resulted from a moderate change in the secondary structure of the DNA/RNA duplexes and a molecular fluctuation in monomers derived from the (*S*)-5′-*C*-aminopropyl side chain, as well as from a variation in sugar puckering derived from the 2′-arabinofluoro modification. Meanwhile, the incorporation of these analogs significantly enhanced the nuclease resistance of the DNA oligomers. Moreover, the (*S*)-5′-*C*-aminopropyl-2′-arabinofluoro-modified DNA/RNA duplexes showed a superior ability to activate RNase H-mediated cleavage of the RNA strand compared to the (*S*)-5′-*C*-aminopropyl-modified DNA/RNA duplexes.

Introduction

Oligonucleotide therapeutics are emerging as a novel solution for treating a variety of genetic and intractable diseases, so-called "undruggable" diseases that cannot be targeted by small molecule or antibody-based drugs.[1] Antisense oligonucleotides (ASOs), which are composed of single-stranded DNA-like oligonucleotides, represent one kind of oligonucleotide therapeutics, and constitute the majority of oligonucleotide therapeutics approved by 2020.[2–6] ASOs are designed to target disease-related pre-mRNAs or mature mRNAs. After forming the DNA/RNA duplexes inside the cells, they are expected to alter the splicing process of pre-mRNAs to control the synthesis of the proteins encoded, or to induce a selective cleavage of the RNA strand processed by ribonuclease H (RNase H), resulting in the prevention of translation into the encoded proteins.[7a–c]

However, there are still some challenges left with regard to ASOs composed of natural monomers (deoxynucleotides or ribonucleotides). It is known that a long half-life of therapeutics is necessary for eliciting sufficient pharmacological effects. In the case of ASOs, the half-life depends on the resistance of these ASOs against numerous nucleases present in the blood circulation. Moreover, it is also essential to reduce the side effects of ASOs by weakening their cytotoxicity, and by enhancing their binding affinity to the target RNAs to suppress off-target effects. As a measure of improving the properties of ASOs, various chemically modified nucleoside analogs have been developed, some of which have already been granted approval for clinical usage. For example, one kind of modification on phosphodiesters, phosphorothioate (PS), which is used in mipomersen and nusinersen, among others, could not only increase the nuclease resistance, but also enhance the intracellular internalization of ASOs, with the cytotoxicity of PS also determined in some of the cases.[2,3,8–10]

As in our previous reports, inserting an aminoalkyl side chain into the 4′- or 5′-site of nucleosides could significantly increase the nuclease resistance of the resulting oligonucleotides.[11–15] Due to the decrease of nuclease resistance when the terminal amino moiety was protected by acetyl groups, it is assumed that the positive charge on the amino moiety of the

[a]*Graduate School of Natural Science and Technology, 1-1 Yanagido, Gifu, 501-1193, Japan. E-mail: uenoy@gifu-u.ac.jp; Fax: +81-58-293-2919; Tel: +81-58-293-2919*
[b]*Faculty of Applied Biological Sciences, 1-1 Yanagido, Gifu, 501-1193, Japan*
[c]*United Graduate School of Agricultural Science, 1-1 Yanagido, Gifu, 501-1193, Japan*
[d]*Center for Highly Advanced Integration of Nano and Life Sciences (G-CHAIN), Gifu University, 1-1 Yanagido, Gifu, 501-1193, Japan*
[e]*Department of Chemical Biology and Applied Chemistry, College of Engineering, Nihon University, 1 Nakagawara, Tokusada, Tamuramachi, Koriyama, Fukushima 963-8642, Japan*

† Electronic supplementary information (ESI) available. See DOI: 10.1039/d0ra08468a

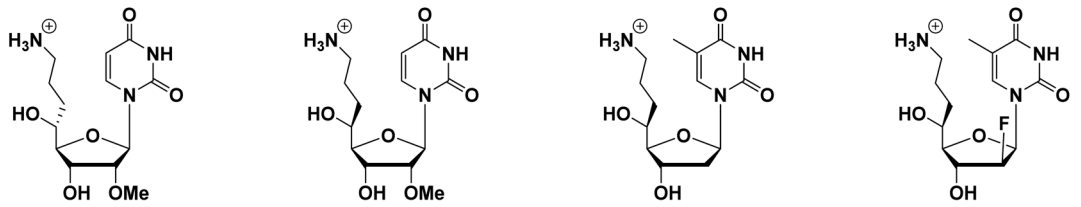

Fig. 1 The chemical structure of (*R*)-5′-aminopropyl-2′-*O*Me-uridine (**A1**), (*S*)-5′-aminopropyl-2′-*O*Me-uridine (**A2**), (*S*)-5′-*C*-aminopropyl-thymidine (**A3**) and (*S*)-5′-*C*-aminopropyl-2′-β-fluoro-thymidine (**A4**).

aminoalkyl side chain acts as an obstacle to nucleases binding to oligonucleotides, and thus inhibits the degradation of oligonucleotides. However, combined with the 2′-*O*-methyl (2′-*O*Me) modification, it was confirmed that the 4′-aminoalkyl modification would cause a decrease in thermal stability, which was related to a deterioration in binding affinity of RNA targets.[12] It was also revealed that the thermal instability could be improved by altering the aminoalkyl side chain from the 4′- to the 5′-site, and, compared with the (*R*)-5′-aminopropyl-2′-*O*Me-modified nucleoside analog (shown in Fig. 1, **A1**), the (*S*)-5′-aminopropyl-2′-*O*Me-modified nucleoside analog (shown in Fig. 1, **A2**), which remained appropriate thermal stability with robust nuclease resistance, was considered the most potent potential candidate for siRNA in our studies so far.[15]

Based on the results obtained by siRNA studies, we addressed whether the (*S*)-5′-aminopropyl modification was also suitable for ASOs to enhance nuclease resistance. However, it was reported that the existence of the 2′-*O*Me modification would act as an obstruction during RNase H-mediated cleavage of the RNA strand.[16,17] Therefore, instead of employing the 2′-*O*Me modification, we focused on the application of the 2′-arabinofluoro (2′-araF or 2′-β-fluoro) modification. The

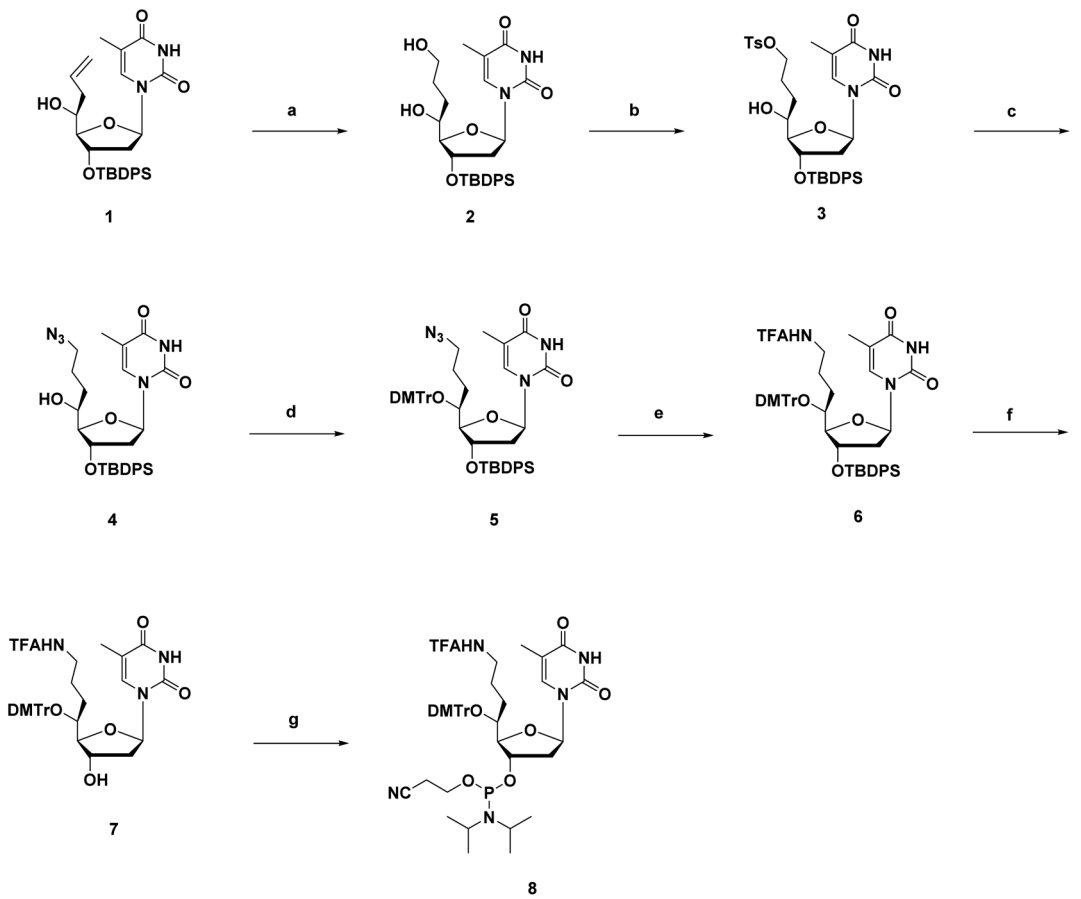

Scheme 1 Synthetic route of (*S*)-5′-*C*-aminopropyl-thymidine phosphoramidite **8**.[a] [a]Reagents and conditions: (a) (1) 9-BBN, THF, r.t., over-night; (2) 2 N NaOH aq., 30% H_2O_2 aq., r.t., 15 min; **2**: quant.; (b) *p*-TsCl, $Me_2N(CH_2)_3NMe_2$, MeCN, −10 °C, 2 h; **3**: 81%; (c) NaN_3, DMF, 60 °C, over-night; **4**: 80%; (d) DMTrOTFA, DIPEA, THF, r.t., 22–24 h; **5**: 91%; (e) (1) Ph_3P, H_2O, THF, 40 °C, 24 h; (2) CF_3CO_2Et, Et_3N, DCM, r.t., over-night; **6**: 89%; (f) TBAF/THF, THF, r.t., 2 h; **7**: 92%; (g) DIPEA, CEPCl, THF, r.t., 1.5 h; **8**: 86%.

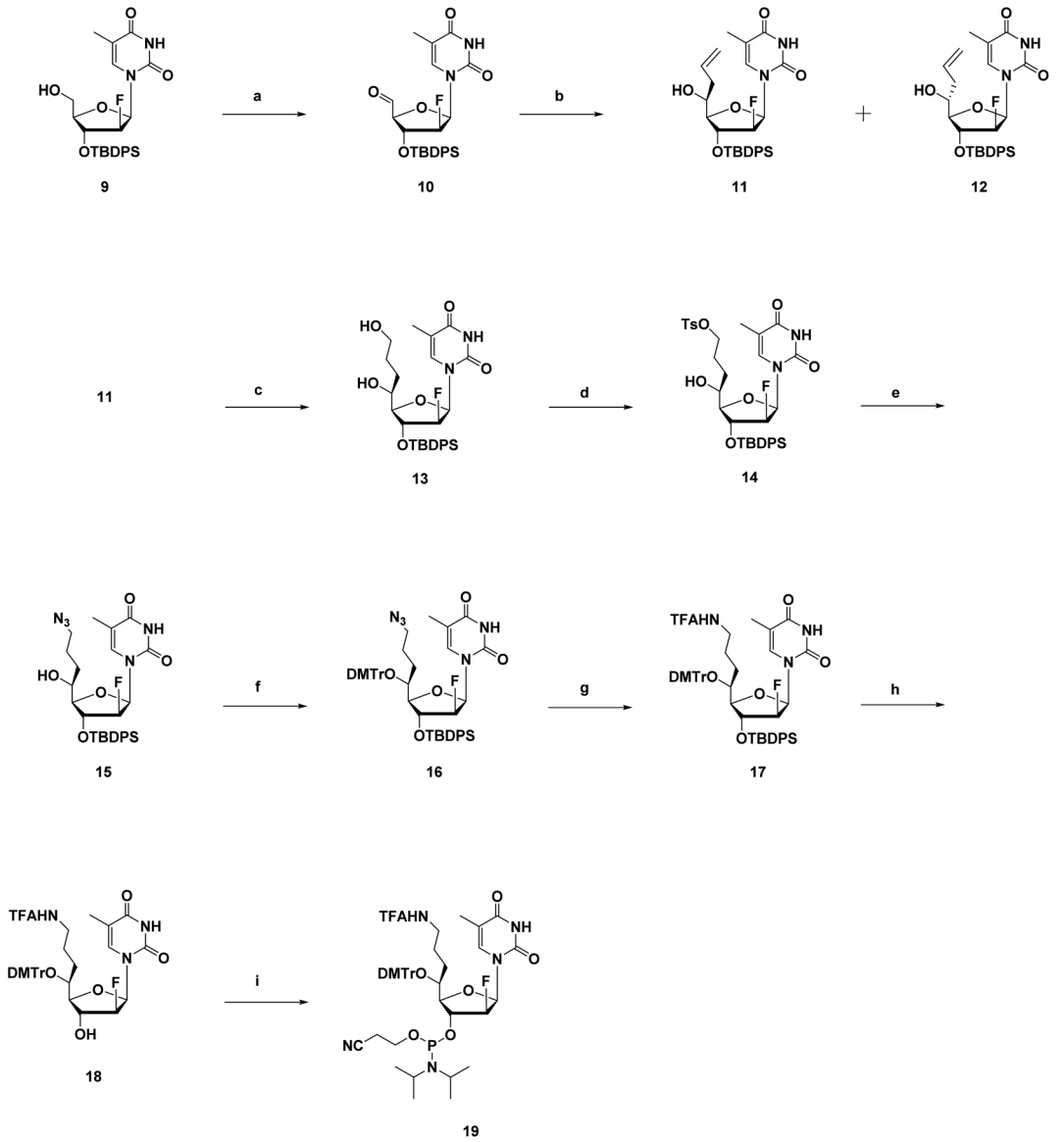

Scheme 2 Synthetic route of (*S*)-5′-*C*-aminopropyl-2′-β-fluoro-thymidine phosphoramidite **19**.[a] [a]Reagents and conditions: (a) EDC·HCl, $CHCl_2CO_2H$, DMSO/DCM (1 : 1 v/v), 0 °C, 3 h; (b) allyltrimethylsilane, $BF_3{\cdot}Et_2O$, DCM, 0 °C, 3 h, **11**: 71% (2 steps); **12**: 4% (2 steps); (c) (1) 9-BBN, THF, r.t., over-night; (2) 2 N NaOH aq., 30% H_2O_2 aq., r.t., 15 min; **13**: 77%; (d) *p*-TsCl, $Me_2N(CH_2)_3NMe_2$, DCM, −10 °C, 2 h; **14**: 81%; (e) NaN_3, DMF, 60 °C, over-night; **15**: 76%; (f) DMTrOTFA, DIPEA, THF, r.t., 22–24 h; **16**: 93%; (g) (1) Ph_3P, H_2O, THF, 40 °C, 24 h; (2) CF_3CO_2Et, Et_3N, DCM, r.t., over-night; **17**: 96%; (h) TBAF/THF, THF, r.t., 2 h; **18**: 95%; (i) DIPEA, CEPCl, THF, r.t., 1.5 h; **19**: 89%.

synthesis and properties of 2′-araF-modified DNAs (FANAs) have been reported by Damha and co-workers.[18] According to these reports, the incorporation of a fluorine atom into the 2′-β-site of the sugar moiety showed no inhibition towards RNase H-mediated cleavage, as well as increased thermal stability of the FANA/RNA duplexes compared with the natural ones.[19,20] In addition, 2′-deoxynucleosides, the natural monomers of DNA, are known not to interfere with the action of RNase H.

In this study, we designed two novel thymidine analogs (Fig. 1): (*S*)-5′-*C*-aminopropyl-thymidine (**A3**) and (*S*)-5′-*C*-aminopropyl-2′-β-fluoro-thymidine (**A4**), envisioning that the dual modification would improve the thermal stability of the DNA/RNA duplexes, and enhance the nuclease resistance of ASOs without inhibiting the cleavage of the RNA strand mediated by RNase H. The following sections outline the synthesis of the nucleoside analogs we designed, and the functional properties of oligonucleotides containing these analogs were further evaluated.

Results and discussion

Synthesis of nucleoside analogs

The synthesis route of phosphoramidites corresponding to (*S*)-5′-*C*-aminopropyl-thymidine (**A3**) is shown in Scheme 1. First, compound **1** was prepared according to a previously reported method.[21,22] Hydroboration and oxidation of the allyl moiety in compound **1** quantitatively produced compound **2**. Next, site-

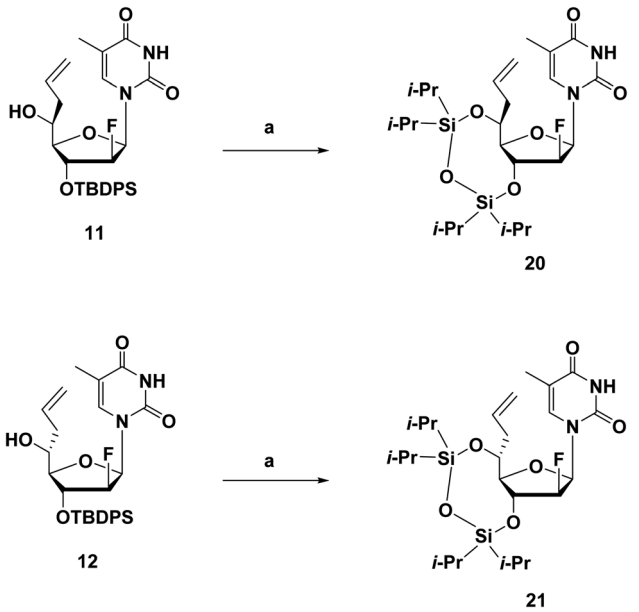

Scheme 3 Synthetic route of the 3′,5′-TIPDS derivatives **20** and **21**.[a] [a]Reagents and conditions: (a) (1) TBAF/THF, THF, r.t., 2 h; (2) $TIPDSCl_2$, pyridine, r.t., 24 h; **20**: 83%; **21**: 87%.

selective tosylation was achieved by controlling the reagent equivalent, which gave compound **3** in 81% yield, and the tosyl group was replaced with the azide group to afford compound **4** in 80% yield. Then, the 5′-hydroxy function, considered as a secondary alcohol, was protected with the DMTr group to give compound **5** in 91% yield, *via* a reported method utilizing DMTrOTFA reagent.[23] After converting the azide groups into an amino function by the Staudinger reaction, the resulting amino function was protected with TFA group to give compound **6** in 89% yield. Finally, deprotection of the 3′-*O*-silyl group of compound **6** by treatment with TBAF afforded compound **7** in 92% yield, followed by a standard phosphorylation procedure to give the corresponding phosphoramidite **8** in 86% yield.

The synthesis route of phosphoramidites corresponding to (*S*)-5′-*C*-aminopropyl-2′-β-fluoro-thymidine (**A4**), similar to that of **A3**, is shown in Scheme 2. Compound **9** was prepared *via* a reported method, followed by oxidization and Hosomi–Sakurai allylation to give compound **11** and **12** in 71% and 4% yield, respectively.[18] Configurations of the 5′-carbons in **11** and **12** were determined *via* nuclear Overhauser effect spectroscopy (NOESY) measurements and ^{1}H NMR. After deprotecting the 3′-*O*-silyl groups of **11** and **12**, the TIPDS group was used to lock the conformations of the sugar moieties of **11** and **12**, resulting in compound **20** and **21** in 83% and 84% yields, respectively (Scheme 3). As a result of the NOESY measurements, the NOE was observed between H-3′ and H-5′ of **21**, but not in **20**, which suggests that compound **11**, the main product generated by Hosomi–Sakurai allylation, was the desired (*S*)-isomer, while compound **12** was the other isomer.[15,24] This conclusions from NOESY measurements were consistent with the results of ^{1}H NMR; the spin–spin coupling constant between H-4′ and H-5′ was measured as 1.84 Hz in **20** and 9.16 Hz in **21**, which suggested the conformation of H-4′ and H-5′ were of the *gauche*- and *anti*-form, respectively. The pure (*S*)-isomer **11** was then converted into compound **13** by hydroboration and oxidation of the allyl moiety, followed by site-selective tosylation of the 5′-hydroxy function to give compound **14** in 81% yield. Notably, the solvent for tosylation of **13** was DCM instead of MeCN due to its poor solubility, which was assumed to result from the incorporation of the fluorine atom. The tosyl group was replaced by azidation to afford compound **15** in 76% yield, followed by the 5′-hydroxy function being protected by the DMTr group to give compound **16** in 93% yield. After converting the azide group into amine by the Staudinger reaction, the resulting amine was protected by TFA group to give compound **17** in 96% yield. Deprotection of the 3′-*O*-silyl group of **17** afforded compound **18** in 95% yield, followed by a standard phosphorylation procedure to give the corresponding phosphoramidite **19** in 89% yield.

Oligonucleotide synthesis

The modified nucleoside analogs **A3** and **A4** were incorporated into DNA oligomers utilizing phosphoramidites **8** and **19**, respectively, by a DNA/RNA synthesizer. After the synthesis, to prevent the additional reaction of acrylonitrile with the 5′-*C*-aminopropyl groups, the CPG beads were treated with 10% dimethylamine in MeCN at room temperature for 5 min, followed by rinsing with MeCN to selectively remove cyanoethyl groups. Then, the DNA oligomers were cleaved from the CPG

Table 1 Sequence of DNA/RNA duplexes, DNAs, RNAs, and T_m values of duplexes

Abbreviation of DNA/RNA duplex	Abbreviation of DNA or RNA	Sequence[a]	T_m[b] (°C)	ΔT_m[c] (°C)	ΔT_m[c] (°C) per mod.
Duplex **1**	DNA **1**	5′-d(TCTTTCTCTTTCCCTT)-3′	60.0	—	—
	RNA **1**	5′-r(AAGGGAAGAGAAAGA)-3′			
Duplex **2**	DNA **2**	5′-d(TC**T**TTC**T**CTTTCCC**T**T)-3′	57.3	−2.7	−0.7
	RNA **1**	5′-r(AAGGGAAGAGAAAGA)-3′			
Duplex **3**	DNA **3**	5′-d(TC*T*TTC*T*CTTTCCC*T*T)-3′	59.1	−0.9	−0.2
	RNA **1**	5′-r(AAGGGAAGAGAAAGA)-3′			

[a] **T** (bold) and *T* (italic) denote (*S*)-5′-*C*-aminopropyl-thymidine (**A3**) and (*S*)-5′-*C*-aminopropyl-2′-β-fluoro-thymidine (**A4**), respectively. [b] The T_m value were measured in 10 mM sodium phosphate buffer (pH 7.0) containing 100 mM NaCl. The concentrations of the duplexes were 3 μM. All measurements were carried out three times, and the data are shown as an average value in Table 1. [c] ΔT_m represents [T_m(duplex **2** or **3**) − T_m(duplex **1**)].

beads and deprotected by treatment with concentrated NH_3 solution for 12 h at 55 °C. The oligomers were purified by 20% denaturing polyacrylamide gel electrophoresis (PAGE) in presence of 7 M urea. The corresponding RNA oligomers used in this study were also prepared by a DNA/RNA synthesizer. In contrast to the DNA oligomers, the RNA oligomers were cleaved from CPG beads and deprotected by treatment with concentrated NH_3 solution/40% methylamine (1 : 1, v/v) for 10 min at 65 °C after the synthesis was complete. Then, 2′-*O*-TBDMS groups in RNA oligomers were removed by incubation with $Et_3N{\cdot}3HF$ (125 μL) in DMSO (100 μL) for 1.5 h at 65 °C. The reaction was quenched with 0.1 M TEAA buffer (pH 7.0), and the mixture was desalted using a Sep-Pak C18 cartridge. Both DNA and RNA oligomers were finally purified by 20% PAGE. The sequences of DNA and RNA used in this study are shown in Tables 1–3, 5, 6, S1 and S2 and Fig. S8.†

Thermal stability of duplexes

To investigate the impact of nucleoside analogs **A3** and **A4** on the thermal stability of the DNA/RNA duplexes, temperature-induced melting was measured by ultraviolet (UV) spectroscopy in 10 mM sodium phosphate buffer (pH 7.0) containing 100 mM NaCl. The 50% melting temperature (T_m) values are shown in Table 1. As a result, the T_m value of the natural DNA/RNA duplex **1** was 60.0 °C, while that of modified duplexes **2** and **3** were 57.3 °C and 59.1 °C, respectively. Additionally, the incorporation of **A3** decreased the T_m value of the duplex by 0.7 °C per modification, while the incorporation of **A4** decreased the T_m value by 0.2 °C per modification, which was considered as stable as the natural duplex **1**. On the other hand, although both **A3** and **A4** showed a slight negative effect on thermal stability, it was revealed that the introduction of the 2′-araF modification improved the thermal stability of the duplexes.

To determine the reason for the difference in T_m in detail, the thermodynamic parameters of duplexes **1–3** were calculated. The thermodynamic parameters from these calculation were based on the slope of a $1/T_m$ *vs.* $\ln(C_T/4)$ plot, where C_T (1, 3, 6, 12, 15, 21, 30 and 60 μM) was the total concentration of each single strand, the results of which are shown in Table 2. The ΔG° value of the natural duplex **1** was −23.0 kcal mol^{-1} at 25 °C and −18.3 kcal mol^{-1} at 37 °C, whereas that of modified duplexes **2** and **3** were −27.4 and −21.6 kcal mol^{-1} at 25 °C, −20.6 and −17.3 kcal mol^{-1} at 37 °C, respectively. The ΔH° value of duplexes **1–3** were −140.0, −196.8 and −129.1 kcal mol^{-1}, while the ΔS° value were −392.6, −568.6 and −360.6 cal mol^{-1} K^{-1}, respectively. These results indicated that the thermal destabilization of duplex **2** was related to the unfavorable entropy, whereas duplex **3** had a more favorable entropy owing to the incorporation of **A4**.

Additionally, the base-discriminating ability of the nucleoside analog **A3** and **A4** in the DNA/RNA duplexes was examined utilizing duplexes **4–15** composed of DNAs **4–6** and RNAs **2–5**. The results obtained are shown in Table 3 and S1† in detail. The ΔT_m values, calculated from [T_m(duplex$_{fully\ matched}$) − T_m(duplex$_{mismatched}$)], of the natural duplexes ranged from −5.3 to −13.8 °C, whereas those of the modified duplexes **8–11** and **12–15** were ranged from −6.0 to −15.8 °C and from −4.0 to −14.6 °C, respectively. These results indicated that the base-

Table 2 Thermodynamic parameters of duplexes[a]

Abbreviation of DNA/RNA duplex	Abbreviation of DNA or RNA	Sequence[b]	ΔH° (kcal mol^{-1})	ΔS° (cal mol^{-1} K^{-1})	ΔG° (kcal mol^{-1})	
Duplex **1**	DNA **1**	5′-d(TCTTTCTCTTTCCCTT)-3′	−140.0	−392.6	−23.0	(25 °C)
	RNA **1**	5′-r(AAGGGAAGAGAAAGA)-3′			−18.3	(37 °C)
Duplex **2**	DNA **2**	5′-d(TC**T**TTC**T**CTTTCCC**T**T)-3′	−196.8	−568.6	−27.4	(25 °C)
	RNA **1**	5′-r(AAGGGAAGAGAAAGA)-3′			−20.6	(37 °C)
Duplex **3**	DNA **3**	5′-d(TC*T*TTC*T*CTTT*C*CC*TT*)-3′	−129.1	−360.6	−21.6	(25 °C)
	RNA **1**	5′-r(AAGGGAAGAGAAAGA)-3′			−17.3	(37 °C)

[a] Thermodynamic parameters were calculated based on the slop of a $1/T_m$ *vs.* $\ln(C_T/4)$ plot. [b] **T** (bold) and *T* (italic) denote (*S*)-5′-*C*-aminopropyl-thymidine (**A3**) and (*S*)-5′-*C*-aminopropyl-2′-β-fluoro-thymidine (**A4**), respectively.

Table 3 Base-discriminating ability of the nucleoside analog A1 and A2 in DNA/RNA duplex[a]

$T_m/\Delta T_m$[b] (°C)					
		Y			
Abbreviation of DNA/RNA duplex	X	A	U	G	C
Duplex **4–7**	Thymidine	47.4 (−)	35.9 (−11.5)	42.1 (−5.3)	33.6 (−13.8)
Duplex **8–11**	**A3**	47.1 (−)	31.3 (−15.8)	41.1 (−6.0)	32.4 (−14.7)
Duplex **12–15**	**A4**	47.3 (−)	34.0 (−13.3)	43.3 (−4.0)	32.7 (−14.6)

[a] The sequences of duplexes are 5′-d(GGCTAXAATGTCG)-3′ for the DNA strand and 5′-r(CGACAUUYUAGCC)-3′ for the RNA strand, shown in Table S1 (see ESI) in detail. Underlined letters denote mismatched base pairs. [b] The T_m value were measured in 10 mM sodium phosphate buffer (pH 7.0) containing 100 mM NaCl. The concentrations the duplexes were 3 μM.

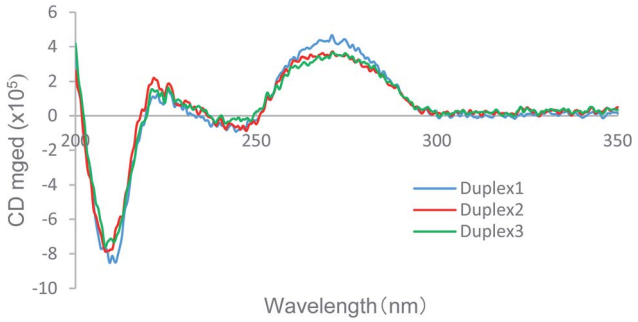

Fig. 2 CD spectra of the native duplex **1** and the modified duplex **2** and **3** in a buffer containing 10 mM sodium phosphate (pH 7.0) and 100 mM NaCl at 25 °C. The concentration of the duplexes was 4 μM.

discriminating abilities of nucleoside analogs **A3** and **A4** were the same as or better than those of the natural ones.

Circular dichroism (CD) spectra

To determine how the incorporation of the nucleoside analogs **A3** and **A4** affected the thermal stability in comparison with the natural ones, CD spectra of the global structures of the duplexes **1–3** was measured, and the results are shown in Fig. 2. It is known that DNA/RNA duplexes adopt an A-type structure with negative and positive peaks at 210 and 270 nm, respectively, consistent with the result for the natural duplex **1**. Since the CD spectra of the modified duplexes **2** and **3** was similar to that of duplex **1**, it is considered that duplexes **2** and **3** form the A-type helix as well. However, the local maxima and minima of the modified duplexes were lower than those of the natural duplex. These variations in CD spectra indicated that there was a moderate change in the secondary structure of the modified duplexes due to the introduction of (*S*)-5′-*C*-aminopropyl modification, which was hence considered the reason for the moderate thermal destabilization observed for the modified duplexes. In addition, the CD spectra of duplexes **2** and **3** were highly similar to each other, resulting in the reverse effect with respect to the entropy values, as revealed by the calculation of the thermodynamic parameters, which was not related to the secondary structure of the duplexes.

Molecular modeling study

In addition to the findings obtained based on the thermodynamic parameters and the CD spectra, the effect of the 2′-araF modification was assumed to play a vital role in determining the thermal stability. It is known that nucleosides adopt the north-type (N-type) *C*3′-endo pucker in DNA/RNA duplexes, which adopt the A-like helix structure. Therefore, it is assumed that there might be a change in sugar pucker resulting from the incorporation of the fluorine atom. To confirm this assumption, the features of nucleoside analogs **A3** and **A4**, together with the natural thymidine, were calculated based on molecular dynamics (MD) simulation.

The root mean square deviations (RMSDs) of heavy atoms were calculated relative to the reference structure attained from the energy minimization calculation (Fig. S1†). As the results shown in Table 4, the wide-range distribution of RMSDs of each nucleoside analog indicates that the fluctuation of the nucleoside analogs was more pronounced than that of the natural thymidine (Fig. S2†), indicating that nucleoside analogs require extra energy while forming duplexes. Next, the time-dependence of sugar puckering was calculated using pseudorotational phase angle (*P*) (Fig. S3†), based on which the percentages in the N-type sugar conformation of each nucleoside were calculated as well. As shown in Table 4, the percentage of **A4** in the N-type sugar conformation was apparently higher than that of the natural one, suggesting that the 2′-araF modification might cause a shift of sugar pucker into the N-type sugar conformation. In addition, the introduction of the (*S*)-5′-*C*-aminopropyl modification has almost no effect on sugar pucker because of the inconspicuous disparity in the N-type abundance ratios of **A3** and thymidine.

Therefore, according to the molecular modeling study, the molecular fluctuation caused by the introduction of the (*S*)-5′-*C*-aminopropyl side chain would result in unfavorable conditions for the DNA/RNA duplex formation and thus cause thermal destabilization, whereas the 2′-arabinofluoro modification suppressed thermal destabilization by preferably adopting the N-type sugar pucker. These molecular modeling-based results were consistent with the findings on the thermodynamic parameters and the CD spectra.

Table 4 The features of thymidine, A3 and A4 obtained from MD simulation

	Thymidine	**A3**	**A4**
RMSD[a] (Å)	0.55 (±0.20)	1.03 (±0.41)	0.83 (±0.33)
N-type[b] (%)	12.5	14.1	19.5

[a] The mean values and standard deviations of RMSD (Å). [b] The percentages of the N-type sugar conformation were calculated based on a criteria that considers the sugar conformation as the N-type if $0° < P < 90°$ and $270° < P < 360°$.

Table 5 The DNA oligomers used in enzymatic stability assays

Abbreviation of DNA	Sequence[a]
DNA **7**	5′-F-d(TCTTTCTCTTTCCCTT)-3′
DNA **8**	5′-F-d(TC**T**TTCTCTTTCCC**T**T)-3′
DNA **9**	5′-F-d(TC*T*TTCTCTTT*C*CC*T*T)-3′

[a] F, **T** (bold) and *T* (italic) denote fluorescein, (*S*)-5′-*C*-aminopropyl-thymidine (**A3**) and (*S*)-5′-*C*-aminopropyl-2′-β-fluoro-thymidine (**A4**), respectively.

Nuclease resistance of DNAs

Since natural nucleotides can easily be disassembled by various nucleases in the blood circulation, it is necessary to enhance the nuclease resistance of oligomers for therapeutic application. To investigate whether the nuclease resistance of DNA oligomers was improved by the incorporation of the nucleoside analogs **A3** and **A4**, an enzymatic stability assay was performed utilizing bovine serum (BS). For this, the fluorescein-labeled single-stranded DNAs **7–9** (Table 5) were dissolved in OPTI-MEM,

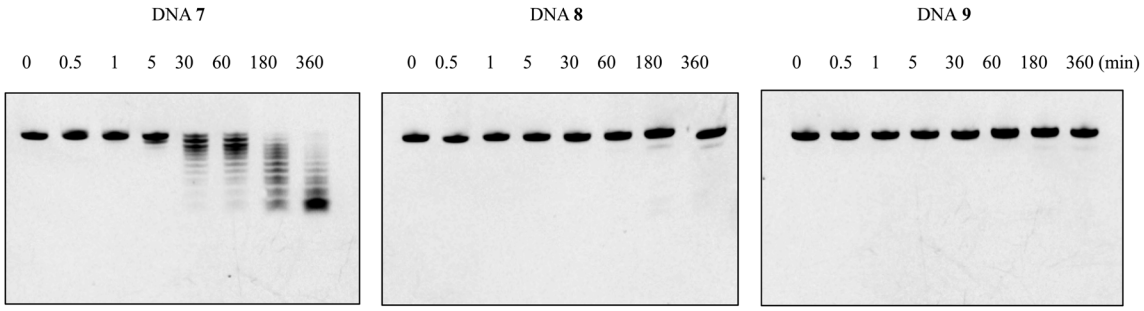

Fig. 3 PAGE analysis of single-stranded DNAs (8 μM) treated in OPTI-MEM containing 3% bovine serum. Fluorescein-labeled DNA **7–9** (300 pmol) were incubated in OPTI-MEM containing 3% bovine serum, and the reaction mixtures at various incubation time (0, 0.5, 1, 5, 30, 60, 180, 360 min) were analyzed by 20% PAGE containing 7 M urea.

and subsequently incubated with 3% BS at 37 °C for the required time. Reaction mixtures were analyzed after various incubation times (0, 0.5, 1, 5, and 30 min, and 1, 3, 6 h) by 20% PAGE in the presence of 7 M urea, and then quantified by Luminescent Image analyzer LAS-4000 (Fujifilm). As shown in Fig. 3, the natural DNA **7** was completely degraded in BS within 3 h of incubation, whereas the modified DNAs **8** and **9** remained >80% and >90% of the complete strand, respectively, even after 6 h of incubation. Therefore, we could show that the incorporation of nucleoside analogs **A3** and **A4** could enhance the nuclease resistance of DNA oligomers. The experimental results were also consistent with previous studies.[15] It is presumed that the positive charges carried by the amino group of the aminopropyl side chain would mask the phosphodiester backbone of the oligomers and electrostatically impede approaching nucleases, thereby improving the nuclease resistance.

The ability for RNase H activation

To investigate whether the modified duplexes containing the nucleoside analogs **A3** and **A4** have the same ability for RNase H activation as the natural ones, RNase H-mediated cleavage assays were performed utilizing RNase H purified from *Escherichia coli*. The natural duplex **16** was composed of DNA **1** and fluorescein-labeled RNA **6**, and the modified duplexes **17** and **18** were composed of DNAs **2** and **3**, respectively, as well as RNA **6** (Table 6). These duplexes were dissolved in a buffer containing 50 mM Tris–HCl (pH 8.0), 75 mM KCl, 3 mM $MgCl_2$ and 10 mM dithiothreitol. Then, diluted RNase H solution (60 unit per L in H_2O) was added, and subsequently the mixture was incubated at 37 °C for the required times (0, 1, 5, 15 and 30 min, and 1, 2, 4 h). The reaction mixtures were analyzed after various incubation times by 20% denaturing PAGE, and then quantified by Luminescent Image analyzer LAS-4000 (Fujifilm). As shown in Fig. 4, after 4 h of incubation, almost no complete strand of RNA **6** remained in the natural duplex **16**, while in duplexes **17** and **18**, the residual prevalence of complete RNA **6** was 88% and 46%, respectively. In other words, compared to the natural oligomer, the incorporation of nucleoside analog **A3** significantly impeded RNase H-mediated cleavage of the RNA strand in the DNA/RNA duplex, while the impact of **A4** was comparatively inconspicuous. According to these results, although the introduction of the (*S*)-5′-*C*-aminopropyl side chain could enhance the nuclease resistance of oligomers considerably, as desired, it might have inhibited the interaction between RNase H and the DNA/RNA duplexes as well. In addition, it was revealed that the combination with the 2′-araF modification could improve the ability to activate RNase H, which was in line with our expectations.

However, it still remains the possibility that the functional properties of the modified duplexes might depend on the number and position of nucleoside analogs. For this reason, DNA **10–13**, which contain only one analog **A4** in different positions, were synthesized. Thermal stability of the DNA/RNA duplexes composed of DNA **10–13** and RNA **1** were evaluated and RNase H-mediated cleavage assays were also performed using the duplexes composed of DNA **10–13** and RNA **6**. The T_m values and images of PAGE analysis were shown in Table S2 and Fig. S8,† respectively. The T_m values indicated that duplexes **19–22** would be thermally stable enough in physiological

Table 6 The DNA/RNA duplexes used in RNase H-dependent cleavage assays

Abbreviation of DNA/RNA duplex	Abbreviation of DNA or RNA	Sequence[a]
Duplex **16**	DNA **1**	5′-d(TCTTTCTCTTTCCCTT)-3′
	RNA **6**	5′-F-r(AAGGGAAGAGAAAGA)-3′
Duplex **17**	DNA **2**	5′-d(TC**T**TTC**T**CTTT**T**CCC**T**T)-3′
	RNA **6**	5′-F-r(AAGGGAAGAGAAAGA)-3′
Duplex **18**	DNA **3**	5′-d(TC*T*TTC*T*CTTT*T*CCC*T*T)-3′
	RNA **6**	5′-F-r(AAGGGAAGAGAAAGA)-3′

[a] **F**, **T** (bold) and *T* (italic) denote fluorescein, (*S*)-5′-*C*-aminopropyl-thymidine (**A3**) and (*S*)-5′-*C*-aminopropyl-2′-β-fluoro-thymidine (**A4**), respectively.

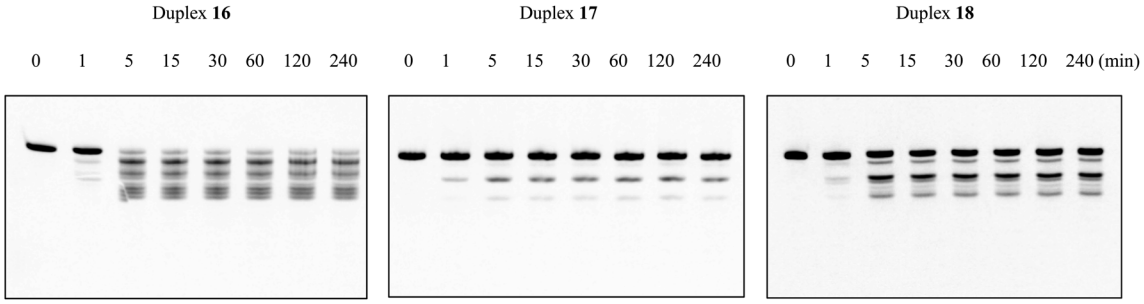

Fig. 4 PAGE analysis of DNA/RNA duplexes treated in a buffer containing 50 mM Tris–HCl (pH 8.0), 75 mM KCl, 3 mM $MgCl_2$, 10 mM dithiothreitol, and RNase H from *E. coli*. The duplex **16–18** were incubated in a buffer containing 50 mM Tris–HCl (pH 8.0), 75 mM KCl, 3 mM $MgCl_2$ and 10 mM dithiothreitol, and then diluted RNase H solution (60 unit per L in H_2O) was added, and subsequently the mixture was incubated at 37 °C for the required time. The reaction mixtures at various incubation time (0, 1, 5, 15, 30, 60, 120, 240 min) were analyzed by 20% PAGE.

conditions, and duplexes **23–26** showed the same behavior as the natural duplex in RNase H-mediated cleavage assays. Meanwhile, it was revealed that the introduction positions of nucleoside analogs should be optimized, and the minimum length of gap, the distance between each nucleoside analog, for RNase H binding should be investigated in further studies.

Conclusions

In summary, this is the first time that the synthesis of (*S*)-5′-*C*-aminopropyl- and (*S*)-5′-*C*-aminopropyl-2′-arabinofluoro-modified thymidines have been accomplished and reported. The properties of the DNA oligomers containing these thymidine analogs were also evaluated. It was revealed that the (*S*)-5′-*C*-aminopropyl-2′-arabinofluoro-thymidine was thermally stable enough compared with the natural one, while the incorporation of (*S*)-5′-*C*-aminopropyl-thymidine caused thermal destabilization. The difference in thermal stability might have resulted from a moderate change in the secondary structure of the DNA/RNA duplexes, as well as a molecular fluctuation in nucleoside structures derived from the introduction of the (*S*)-5′-*C*-aminopropyl side chain, and the variation in sugar pucker derived from the 2′-arabinofluoro modification. Meanwhile, the incorporation of these nucleoside analogs could significantly enhance the nuclease resistance of DNA oligomers exposed to BS. Moreover, the DNA/RNA duplexes containing the (*S*)-5′-*C*-aminopropyl-2′-arabinofluoro-thymidine showed a superior ability to activate RNase H-mediated cleavage of the RNA strand. Hence, the (*S*)-5′-*C*-aminopropyl-2′-arabinofluoro-modified nucleoside analogs might be potential candidates for the application of RNase H-dependent antisense oligonucleotides as therapeutics, although the introduction position should be optimized, and their cytotoxicity and cell membrane permeability need to be evaluated in further studies.

Experimental section

General remark

All chemicals and dry solvents (DCE, DCM, DMF, MeCN, THF, and pyridine) were obtained from commercial sources and used without any further purification. Thin layer chromatography (TLC) was performed on silica gel plates precoated with fluorescent indicator with visualization by UV light or by dipping into a solution of 5% (v/v) concentrated H_2SO_4 in a mixture of *p*-anisaldehyde and methanol, and then heating. Silica gel (63–210 mesh) was used for column chromatography. ^{1}H NMR (400 or 500 MHz), ^{13}C {1H} NMR (101 MHz), ^{19}F NMR (376 MHz), ^{31}P NMR (162 MHz) were recorded on 400 or 500 MHz NMR equipment. Acetonitrile-d_3, $CDCl_3$, or DMSO-d_6 was used as a solvent for obtaining NMR spectra. Chemical shifts (δ) are given in parts per million (ppm) from $CDCl_3$ (7.26 ppm) for ^{1}H NMR spectra and $CDCl_3$ (77.2 ppm) for ^{13}C NMR spectra. The abbreviations s, d, t, q, and m signify singlet, doublet, triplet, quadruplet, and multiplet, respectively. High resolution mass spectra (HRMS) were obtained in positive ion electrospray ionization (ESI-TOF) mode. The purity of each oligomers which were synthesized in this study was confirmed by HPLC and MALDI-TOF/MS.

3′-*O*-[(1,1-Dimethylethyl)diphenylsilyl]-(*S*)-5′-*C*-hrdroxypropyl-thymidine (2)

9-Borabicyclo[3.3.1]nonane (9-BBN, 0.5 M in THF, 62 mL) was added dropwise to a solution of compound **1** (2.69 g, 5.16 mmol) in THF (27 mL) under argon atmosphere at 0 °C, and the reactant was stirred for 17 h at room temperature. Then, 2 N NaOH solution (46 mL) and 30% aqueous hydrogen peroxide solution (11 mL) were added dropwise to the reactant in turn. After stirring for 15 min, the reactant was quenched with 30% $Na_2S_2O_3$ solution, and extracted with ethyl acetate and water; the organic layer was washed with brine, dried by Na_2SO_4, filtered and concentrated. The crude material was purified by column chromatography (80% ethyl acetate in hexane) to afford desired product **2** as a white solid (3.78 g, quant.). ^{1}H NMR (400 MHz, $CDCl_3$) δ: 1.08 (s, 9H), 1.42–1.62 (m, 4H), 1.85 (d, J = 0.92 Hz, 3H), 2.23 (m, 2H), 3.08–3.10 (m, 1H), 3.52–3.65 (m, 2H), 3.80 (t, J = 2.3 Hz, 1H), 4.46 (d, J = 1.8 Hz, 1H), 6.24 (t, J = 6.9 Hz, 1H), 7.37–7.47 (m, 6H), 7.49 (d, J = 0.92 Hz, 1H), 7.62–7.66 (m, 4H), 8.54 (s, 1H); ^{13}C{^{1}H} NMR (101 MHz, $CDCl_3$) δ: 12.6, 19.2, 27.1, 29.2, 31.9, 39.9, 63.0, 71.2, 74.9, 87.5, 90.3, 111.0, 128.0, 130.2, 133.3, 133.6, 135.9, 136.0, 137.7, 150.5, 163.7; HRMS (ESI-TOF) *m*/*z* calcd for $C_{29}H_{38}N_2NaO_6Si$ $[M + Na]^+$, 561.2397, found 561.2371.

3′-*O*-[(1,1-Dimethylethyl)diphenylsilyl]-(*S*)-5′-*C*-*p*-toluenesulfonyloxypropyl-thymidine (3)

p-Toluenesulfonyl chloride (*p*-TsCl, 0.111 g, 0.58 mmol) was added to a solution of compound **2** (0.201 g, 0.37 mmol) in MeCN (2.00 mL) under argon atmosphere at 0 °C, and the mixture was stirred at −10 °C while $Me_2N(CH_2)_3NMe_2$ (0.09 mL, 0.56 mmol) being added. The reactant was stirred for 2 h at −10 °C, and then extracted with ethyl acetate and saturated $NaHCO_3$; the organic layer was washed with brine, dried by Na_2SO_4, filtered and concentrated. The crude material was purified by column chromatography (50% ethyl acetate in hexane) to afford desired product **3** as a white solid (0.204 g, 81%). ^{1}H NMR (400 MHz, $CDCl_3$) δ: 1.07 (s, 9H), 1.24–1.43 (m, 2H), 1.50–1.67 (m, 2H), 1.86 (s, 3H), 2.18–2.35 (m, 3H), 2.44 (s, 3H), 2.96–3.00 (m, 1H), 3.72 (t, J = 2.3 Hz, 1H), 3.89–3.99 (m, 2H), 4.42–4.43 (m, 1H), 6.11 (dd, J = 5.9 Hz, 8.3 Hz, 1H), 7.25 (d, J = 1.4 Hz, 1H), 7.32–7.48 (m, 8H), 7.60–7.65 (m, 4H), 7.76 (d, J = 8.2 Hz, 2H), 8.63 (s, 1H); ^{13}C{^{1}H} NMR (101 MHz, $CDCl_3$) δ: 12.6, 19.1, 21.8, 25.4, 27.0, 30.2, 39.4, 70.4, 74.4, 88.5, 89.8, 111.2, 128.0, 128.06, 128.11, 130.0, 130.2, 130.4, 133.1, 133.2, 135.8, 135.9, 137.9, 144.9, 150.4, 163.7; HRMS (ESI-TOF) *m*/*z* calcd for $C_{36}H_{44}N_2NaO_8SSi$ [M + Na]$^+$, 715.2485, found 715.2514.

(*S*)-5′-*C*-Azidopropyl-3′-*O*-[(1,1-dimethylethyl)diphenylsilyl]-thymidine (4)

Sodium azide (0.137 g, 2.45 mmol) was added in a solution of compound **3** (0.204 g, 0.29 mmol) in DMF (2.0 mL) under argon atmosphere. The reactant was stirred for 20 h at 60 °C, and then extracted with ethyl acetate and water; the organic layer was washed with brine, dried by Na_2SO_4, filtered and concentrated. The crude material was purified by column chromatography (50% ethyl acetate in hexane) to afford desired product **4** as a white solid (0.132 g, 80%). ^{1}H NMR (400 MHz, $CDCl_3$) δ: 1.09 (s, 9H), 1.30–1.61 (m, 4H), 1.87 (d, J = 0.92 Hz, 3H), 2.20–2.37 (m, 2H), 2.50 (bs, 1H), 3.02 (s, 1H), 3.15–3.25 (m, 2H), 3.76 (t, J = 2.3 Hz, 1H), 4.44–4.47 (m, 1H), 6.13 (dd, J = 6.0 Hz, 8.3 Hz, 1H), 7.28 (d, J = 0.92 Hz, 1H), 7.38–7.49 (m, 6H), 7.61–7.67 (m, 4H), 8.68 (s, 1H); ^{13}C{^{1}H} NMR (101 MHz, $CDCl_3$) δ: 12.6, 19.2, 25.3, 27.0, 31.5, 39.5, 51.3, 70.6, 74.5, 88.5, 89.8, 111.2, 128.1, 130.2, 130.3, 133.1, 133.5, 135.8, 135.9, 137.8, 150.4, 163.7; HRMS (ESI-TOF) *m*/*z* calcd for $C_{29}H_{37}N_5NaO_5Si$ [M + Na]$^+$, 586.2462, found 586.2483.

(*S*)-5′-*C*-Azidopropyl-5′-*O*-[bis(4-methoxyphenyl) phenylmethyl]-3′-*O*-[(1,1-dimethylethyl)diphenylsilyl]-thymidine (5)

Trifluoroacetic anhydride (0.80 mL, 5.61 mmol) was added in a solution of 4,4′-dimethoxytrityl alcohol (DMTrOH, 1.50 g, 4.68 mmol) in DCM (12 mL) under argon atmosphere. The reactant was stirred for 2.5 h at room temperature and then concentrated. The residue was dissolved with THF (4 mL) and added in a mixture of compound **4** (1.05 g, 1.87 mmol) and *N*,*N*-diisopropylethylamine (DIPEA, 1.00 mL, 5.80 mmol) in THF (2 mL). The reactant was stirred for 22 h at room temperature and then extracted with ethyl acetate and saturated $NaHCO_3$; the organic layer was washed with brine, dried by Na_2SO_4, filtered and concentrated. The crude material was purified by column chromatography (33% ethyl acetate in hexane) to afford desired product **5** as a yellow solid (1.48 g, 91%). ^{1}H NMR (400 MHz, $CDCl_3$) δ: 0.55–0.65 (m, 1H), 1.00 (s, 9H), 1.04–1.10 (m, 1H), 1.12–1.20 (m, 1H), 1.50–1.57 (m, 1H), 1.78 (d, J = 0.92 Hz, 3H), 2.14–2.38 (m, 2H), 2.74–2.93 (m, 3H), 3.77 (s, 3H), 3.77 (s, 3H), 3.84 (s, 1H), 4.41 (d, J = 6.0 Hz, 1H), 6.50 (dd, J = 5.5 Hz, 9.2 Hz, 1H), 6.67 (t, J = 8.7 Hz, 4H), 7.04–7.51 (m, 19H), 7.86 (d, J = 1.4 Hz, 1H), 8.26 (s, 1H); ^{13}C{^{1}H} NMR (101 MHz, $CDCl_3$) δ: 12.5, 19.0, 25.0, 26.9, 28.7, 41.7, 51.1, 55.4, 74.8, 75.2, 84.7, 87.4, 87.9, 111.4, 113.1, 127.1, 127.9, 128.0, 128.2, 130.3, 130.4, 135.6, 135.8, 146.0, 150.3, 158.7, 163.6; HRMS (ESI-TOF) *m*/*z* calcd for $C_{50}H_{55}N_5NaO_7Si$ [M + Na]$^+$, 888.3768, found 888.3739.

(*S*)-5′-*O*-[Bis(4-methoxyphenyl)phenylmethyl]-3′-*O*-[(1,1-dimethylethyl)diphenylsilyl]-5′-*C*-trifluoroacetylaminopropyl-thymidine (6)

Triphenylphosphine (0.313 g, 1.19 mmol) and water (0.33 mL) were added in a solution of compound **5** (0.340 g, 0.46 mmol) in THF (7.80 mL). The reactant was stirred for 24 h at 40 °C and then concentrated. The residue was dissolved with DCM (4.6 mL), and then triethylamine (0.10 mL, 0.69 mmol) and CF_3-CO_2Et (0.16 mL, 1.38 mmol) were added in turn. After being stirred for 17 h at room temperature, the reactant was extracted with ethyl acetate and water; the organic layer was washed with brine, dried by Na_2SO_4, filtered and concentrated. The crude material was purified by column chromatography (50% ethyl acetate in hexane) to afford desired product **6** as a yellow solid (0.385 g, 89%). ^{1}H NMR (400 MHz, $CDCl_3$) δ: 0.54–0.65 (m, 1H), 0.91–1.15 (m, 2H), 1.00 (s, 9H), 1.49–1.52 (m, 1H), 1.63 (s, 2H) 1.79 (d, J = 0.92 Hz, 3H), 2.17–2.39 (m, 2H), 2.85–2.94 (m, 3H), 3.77 (s, 3H), 3.78 (s, 3H), 3.79 (s, 1H), 4.42 (d, J = 5.5 Hz, 1H), 6.06 (s, 1H), 6.50 (dd, J = 5.0 Hz, 9.2 Hz, 1H), 6.65–6.69 (m, 4H), 7.04–7.49 (m, 19H), 7.85 (d, J = 0.92 Hz, 1H), 8.39 (s, 1H); ^{13}C{^{1}H} NMR (101 MHz, $CDCl_3$) δ: 12.5, 19.0, 24.7, 26.9, 28.5, 39.7, 41.5, 55.4, 74.6, 75.2, 84.8, 87.4, 87.8, 111.5, 113.2, 127.2, 127.8, 128.0, 128.2, 130.0, 130.1, 130.2, 130.4, 135.7, 135.8, 145.8, 150.3, 158.75, 158.82, 163.6; HRMS (ESI-TOF) *m*/*z* calcd for $C_{52}H_{56}F_3N_3NaO_8Si$ [M + Na]$^+$, 958.3686, found 958.3659.

(*S*)-5′-*O*-[Bis(4-methoxyphenyl)phenylmethyl]-5′-*C*-trifluoroacetylaminopropyl-thymidine (7)

Tetrabutylammonium fluoride (TBAF, 3.20 mL of a 1 M solution in THF) was added in a solution of compound **6** (1.39 g, 1.49 mmol) in THF (32 mL) under argon atmosphere, and the reactant was stirred for 2 h at room temperature. The reactant was extracted with ethyl acetate and saturated $NaHCO_3$; the organic layer was washed with brine, dried by Na_2SO_4, filtered and concentrated. The crude material was purified by column chromatography (75% ethyl acetate in hexane) to afford desired product **7** as a white solid (0.922 g, 92%). ^{1}H NMR (400 MHz, DMSO-d_6) δ: 1.00–1.05 (m, 1H), 1.19–1.31 (m, 3H), 1.68 (s, 3H), 2.09–2.15 (m, 1H), 2.20–2.27 (m, 1H), 2.81–2.82 (m, 2H), 3.25–3.26 (m, 1H), 3.73 (s, 3H), 3.74 (s, 3H), 3.77 (t, J = 3.7 Hz, 1H), 4.14–4.17 (m, 1H), 5.19 (d, J = 5.0 Hz, 1H), 6.15 (t, J = 6.4 Hz, 1H), 6.86 (t, J = 8.7 Hz, 4H), 7.18–7.42 (m, 9H), 7.68 (s, 1H), 9.21

(t, J = 6.0 Hz, 1H), 11.38 (s, 1H); $^{13}C\{^1H\}$ NMR (101 MHz, DMSO-d_6) δ: 12.1, 24.1, 27.9, 55.0, 70.4, 73.8, 79.2, 83.4, 86.2, 86.7, 109.7, 113.0, 126.7, 127.6, 127.8, 130.0, 130.1, 135.4, 136.2, 136.5, 146.3, 158.1, 158.2, 163.7; HRMS (ESI-TOF) m/z calcd for $C_{36}H_{38}F_3N_3NaO_8$ $[M + Na]^+$, 720.2509, found 720.2481.

3′-*O*-[2-Cyanoethoxy(diisopropylamino)phosphino]-(*S*)-5′-*O*-[bis(4-methoxyphenyl)phenylmethyl]-5′-*C*-trifluoroacetylaminopropyl-thymidine (8)

N,*N*-Diisopropylethylamine (DIPEA, 0.64 mL, 3.66 mmol) and 2-cyanoethyl *N*,*N*-diisopropylchlorophosphoramidite (CEPCl, 0.32 mL, 1.44 mmol) were added in a solution of compound **7** (0.500 g, 0.72 mmol) in THF (5.00 mL) in turn under argon atmosphere. The reactant was stirred for 1.5 h at room temperature, and then extracted with ethyl acetate and saturated $NaHCO_3$; the organic layer was washed with brine, dried by Na_2SO_4, filtered and concentrated. The crude material was purified by column chromatography (60% ethyl acetate in hexane) to afford desired product **8** as a white solid (0.556 g, 86%). ^{31}P NMR (162 MHz, $CDCl_3$) δ: 148.9, 150.4; HRMS (ESI-TOF) m/z calcd for $C_{45}H_{55}F_3N_5NaO_9P$ $[M + Na]^+$, 920.3587, found 920.2581.

(*S*)-5′-*C*-Allyl-3′-*O*-[(1,1-dimethylethyl)diphenylsilyl]-2′-β-fluoro-thymidine (11) and (*R*)-5′-*C*-allyl-3′-*O*-[(1,1-dimethylethyl)diphenylsilyl]-2′-β-fluoro-thymidine (12)

50% DMSO in DCM (44 mL) was added to a mixture of compound **9** (4.38 g, 8.79 mmol) and 1-(3-(dimethylamino) propyl)-3-ethylcarbodiimide hydrochloride (EDC·HCl, 6.75 g, 35.2 mmol) under argon atmosphere, and the mixture was stirred at 0 °C. Then, $CHCl_2CO_2H$ (0.36 mL, 4.40 mmol) was added dropwise to the mixture and stirred for 3 h at 0 °C. The reactant was extracted with ethyl acetate and saturated $NaHCO_3$; the organic layer was washed with brine, dried by Na_2SO_4, filtered and concentrated. The residue was dissolved in DCM (87 mL) under argon atmosphere, and the mixture was stirred at 0 °C. Then, allyltrimethylsilane (7.00 mL, 44.11 mmol) and boron trifluoride-ethyl ether complex (5.00 mL, 39.81 mmol) were added to the mixture. The reactant was stirred for 4 h at 0 °C, then extracted with ethyl acetate and saturated $NaHCO_3$; the organic layer was washed with brine, dried by Na_2SO_4, filtered and concentrated. The crude material was purified by column chromatography (28.5% ethyl acetate in hexane) to afford desired product **11**, of which the R_f value on TLC was little lower than that of another product **12**, as a white solid (3.36 g, 71%). ^1H NMR (400 MHz, $CDCl_3$) δ: 1.10 (s, 9H), 1.41 (d, J = 5.5 Hz, 1H), 1.88 (s, 3H), 2.01–2.11 (m, 1H), 2.31–2.35 (m, 1H), 3.56 (s, 1H), 3.89 (dd, J = 2.1 Hz, 7.1 Hz, 1H), 4.54 (d, J = 15.1 Hz, 1H), 4.83 (dd, J = 2.3 Hz, 51.3 Hz, 1H), 5.10–5.22 (m, 2H), 5.67–5.78 (m, 1H), 6.30 (q, J = 2.5 Hz, 22.7 Hz, 1H), 7.18 (s, 1H), 7.40–7.49 (m, 6H), 7.65–7.69 (m, 4H), 8.29 (s, 1H).

Another product **12** as a white solid (0.188 g, 4%).^1H NMR (400 MHz, $CDCl_3$) δ:1.10 (s, 9H), 1.56 (broad s, 1H), 1.86 (d, J = 1.2 Hz, 3H), 2.05–2.10 (m, 2H), 3.21–3.26 (m, 1H), 3.80 (t, J = 4.0 Hz, 1H), 4.39–4.46 (m, 1H), 4.96–5.11 (m, 3H), 5.58–5.68 (m, 1H), 6.30 (dd, J = 3.8 Hz, 18.6 Hz, 1H), 7.32 (s, 1H), 7.40–7.70 (m, 10H), 8.07 (broad s, 1H).

3′-*O*-[(1,1-Dimethylethyl)diphenylsilyl]-2′-β-fluoro-(*S*)-5′-*C*-hrdroxypropyl-thymidine (13)

9-Borabicyclo[3.3.1]nonane (9-BBN, 0.5 M in THF, 75 mL) was added dropwise to a solution of compound **11** (3.36 g, 6.24 mmol) in THF (30 mL) under argon atmosphere at 0 °C, and the reactant was stirred for 17 h at room temperature. Then, 2 N NaOH solution (40 mL) and 30% aqueous hydrogen peroxide solution (13 mL) were added dropwise to the reactant in turn. After stirring for 15 min, the reactant was quenched with 30% $Na_2S_2O_3$ solution, and extracted with ethyl acetate and water; the organic layer was washed with brine, dried by Na_2SO_4, filtered and concentrated. The crude material was purified by column chromatography (67% ethyl acetate in hexane) to afford desired product **13** as a white solid (2.67 g, 77%). ^1H NMR (400 MHz, $CDCl_3$) δ: 1.09 (s, 9H), 1.34–1.43 (m, 2H), 1.51–1.58 (m, 2H), 1.85 (s, 3H), 3.24–3.26 (m, 1H), 3.52–3.63 (m, 2H), 3.78 (t, J = 4.1 Hz, 1H), 4.37–4.41 (m, 1H), 4.95–5.08 (m, 1H), 6.30 (dd, J = 3.7 Hz, 18.8 Hz, 1H), 7.35 (s, 1H), 7.40–7.48 (m, 6H), 7.64–7.67 (m, 4H), 8.88 (s, 1H); $^{13}C\{^1H\}$ NMR (101 MHz, $CDCl_3$) δ: 12.6, 19.2, 27.0, 29.1, 30.8, 62.7, 70.0, 76.3, 76.6, 77.4, 83.4, 83.5, 87.3, 94.4, 96.3, 110.3, 128.15, 128.21, 130.5, 132.3, 132.6, 135.9, 136.0, 137.0, 150.3, 163.8; ^{19}F NMR (376 MHz, $CDCl_3$) δ: −120.91 (t, J = 23.09 Hz, 34.67 Hz); HRMS (ESI-TOF) m/z calcd for $C_{29}H_{37}FN_2NaO_6Si$ $[M + Na]^+$, 579.2303, found 579.2296.

3′-*O*-[(1,1-Dimethylethyl)diphenylsilyl]-2′-β-fluoro-(*S*)-5′-*C*-*p*-toluenesulfonyloxypropyl-thymidine (14)

p-Toluenesulfonyl chloride (*p*-TsCl, 0.588 g, 3.08 mmol) was added to a solution of compound **13** (1.13 g, 2.03 mmol) in DCM (11.5 mL) under argon atmosphere at 0 °C, and the mixture was stirred at −10 °C while $Me_2N(CH_2)_3NMe_2$ (0.51 mL, 3.05 mmol) being added. The reactant was stirred for 2 h at −10 °C, and then extracted with ethyl acetate and saturated $NaHCO_3$; the organic layer was washed with brine, dried by Na_2SO_4, filtered and concentrated. The crude material was purified by column chromatography (40% ethyl acetate in hexane) to afford desired product **14** as a white solid (0.204 g, 81%). ^1H NMR (400 MHz, $CDCl_3$) δ: 1.09 (s, 9H), 1.22–1.38 (m, 2H), 1.49–1.73 (m, 3H), 1.85 (d, J = 0.88 Hz, 3H), 2.44 (s, 3H), 3.08–3.12 (m, 1H), 3.70 (t, J = 3.6 Hz, 1H), 3.93–3.96 (m, 2H), 4.33 (m, 1H), 5.02 (m, 1H), 6.28 (dd, J = 3.7 Hz, 19.2 Hz, 1H), 7.27 (s, 1H), 7.33–7.51 (m, 8H), 7.62–7.67 (m, 4H), 7.75–7.79 (m, 2H), 8.78 (s, 1H); $^{13}C\{^1H\}$ NMR (101 MHz, $CDCl_3$) δ: 12.6, 19.2, 21.8, 25.5, 27.0, 29.4, 69.6, 70.2, 76.2, 76.5, 83.3, 83.5, 87.1, 94.3, 96.3, 110.5, 128.0, 128.3, 130.0, 130.6, 130.7, 132.2, 132.5, 133.2, 135.8, 136.0, 136.8, 145.0, 150.3, 163.6; ^{19}F NMR (376 MHz, $CDCl_3$) δ: −120.16 (d, J = 34.67 Hz); HRMS (ESI-TOF) m/z calcd for $C_{36}H_{43}FN_2NaO_8Si$ $[M + Na]^+$, 733.2391, found 733.2401.

(*S*)-5′-*C*-Azidopropyl-3′-*O*-[(1,1-dimethylethyl)diphenylsilyl]-2′-β-fluoro-thymidine (15)

Sodium azide (0.424 g, 7.56 mmol) was added in a solution of compound **14** (0.633 g, 0.89 mmol) in DMF (6.5 mL) under

argon atmosphere. The reactant was stirred for 22 h at 60 °C, and then extracted with ethyl acetate and water; the organic layer was washed with brine, dried by Na_2SO_4, filtered and concentrated. The crude material was purified by column chromatography (40% ethyl acetate in hexane) to afford desired product **15** as a white solid (0.392 g, 76%). ^{1}H NMR (400 MHz, $CDCl_3$) δ: 1.10 (s, 9H), 1.23–1.69 (m, 4H), 1.75 (s, 1H), 1.86 (d, J = 0.92 Hz, 3H), 3.15–3.25 (m, 3H), 3.75 (t, J = 4.1 Hz, 1H), 4.36 (ddd, J = 1.8 Hz, 4.1 Hz, 18.8 Hz, 1H), 5.03 (ddd, J = 1.8 Hz, 3.2 Hz, 52.2 Hz, 1H), 6.32 (dd, J = 3.2 Hz, 19.2 Hz, 1H), 7.27 (s, 1H), 7.41–7.52 (m, 6H), 7.64–7.68 (m, 4H), 8.99 (s, 1H); ^{13}C{^{1}H} NMR (101 MHz, $CDCl_3$) δ: 12.7, 19.2, 25.3, 27.0, 30.7, 51.2, 69.7, 76.3, 76.5, 83.3, 83.5, 87.0, 94.4, 96.3, 110.5, 128.2, 128.3, 130.61, 130.64, 132.6, 132.6, 135.9, 136.0, 136.7, 150.3, 163.7; ^{19}F NMR (376 MHz, $CDCl_3$) δ: −121.09 (d, J = 69.33 Hz); HRMS (ESI-TOF) m/z calcd for $C_{29}H_{36}FN_5NaO_5Si$ $[M + Na]^+$, 604.2367, found 604.2351.

(*S*)-5′-*C*-Azidopropyl-5′-*O*-[bis(4-methoxyphenyl) phenylmethyl]-3′-*O*-[(1,1-dimethylethyl)diphenylsilyl]-2′-β-fluoro-thymidine (16)

Trifluoroacetic anhydride (0.95 mL, 6.81 mmol) was added in a solution of 4,4′-dimethoxytrityl alcohol (DMTrOH, 1.86 g, 5.82 mmol) in DCM (18 mL) under argon atmosphere. The reactant was stirred for 2.5 h at room temperature and then concentrated. The residue was dissolved with THF (5 mL) and added in a mixture of compound **15** (1.03 g, 2.27 mmol) and *N*,*N*-diisopropylethylamine (DIPEA, 1.20 mL, 6.96 mmol) in THF (2 mL). The reactant was stirred for 24 h at room temperature and then extracted with ethyl acetate and saturated $NaHCO_3$; the organic layer was washed with brine, dried by Na_2SO_4, filtered and concentrated. The crude material was purified by column chromatography (33% ethyl acetate in hexane) to afford desired product **16** as a yellow solid (1.87 g, 93%). ^{1}H NMR (400 MHz, $CDCl_3$) δ: 0.71–0.80 (m, 1H), 1.00 (s, 9H), 1.10–1.21 (m, 2H), 1.39–1.50 (m, 1H), 1.78 (d, J = 0.92 Hz, 3H), 2.74–2.91 (m, 2H), 3.20–3.22 (m, 1H), 3.78 (s, 3H), 3.78 (s, 3H), 3.97 (dd, J = 2.5 Hz, 4.1 Hz, 1H), 4.69 (dd, J = 4.1 Hz, 20.6 Hz, 1H), 5.02 (dd, J = 3.2 Hz, 51.8 Hz, 1H), 6.26 (dd, J = 3.2 Hz, 20.6 Hz, 1H), 6.67–6.72 (m, 4H), 7.12–7.17 (m, 7H), 7.27–7.56 (m, 11H), 7.59 (d, J = 1.4 Hz, 1H), 8.70 (s, 1H); ^{13}C{^{1}H} NMR (101 MHz, $CDCl_3$) δ: 12.6, 19.2, 25.0, 26.9, 28.7, 51.2, 55.3, 73.1, 77.4, 83.1, 83.3, 85.7, 86.4, 95.5, 97.4, 110.2, 113.1, 126.9, 127.7, 128.06, 128.10, 128.3, 130.3, 130.4, 132.2, 132.4, 135.7, 135.7, 136.4, 136.8, 137.5, 146.1, 150.2, 158.6, 158.7, 163.7; ^{19}F NMR (376 MHz, $CDCl_3$) δ: −119.02 (t, J = 23.12 Hz, 46.21 Hz); HRMS (ESI-TOF) m/z calcd for $C_{50}H_{54}FN_5NaO_7Si$ $[M + Na]^+$, 906.3674, found 906.3688.

(*S*)-5′-*O*-[Bis(4-methoxyphenyl)phenylmethyl]-3′-*O*-[(1,1-dimethylethyl)diphenylsilyl]-2′-β-fluoro-5′-*C*-trifluoroacetylaminopropyl-thymidine (17)

Triphenylphosphine (1.39 g, 5.31 mmol) and water (1.50 mL) were added in a solution of compound **16** (1.87 g, 2.11 mmol) in THF (37.5 mL). The reactant was stirred for 24 h at 40 °C and then concentrated. The residue was dissolved with DCM (420 mL), and then triethylamine (0.44 mL, 3.17 mmol) and CF_3-CO_2Et (0.76 mL, 6.33 mmol) were added in turn. After being stirred for 17 h at room temperature, the reactant was extracted with ethyl acetate and water; the organic layer was washed with brine, dried by Na_2SO_4, filtered and concentrated. The crude material was purified by column chromatography (40% ethyl acetate in hexane) to afford desired product **17** as a yellow solid (1.93 g, 96%). ^{1}H NMR (400 MHz, $CDCl_3$) δ: 0.70–0.75 (m, 1H), 0.99 (s, 9H), 1.07–1.17 (m, 2H), 1.32–1.40 (m, 1H), 1.78 (d, J = 0.92 Hz, 3H), 2.90 (dd, J = 6.4 Hz, 12.8 Hz, 2H), 3.17–3.19 (m, 1H), 3.77 (s, 3H), 3.78 (s, 3H), 3.94 (dd, J = 2.7 Hz, 3.7 Hz, 1H), 4.68 (dd, J = 3.7 Hz, 20.2 Hz, 1H), 5.02 (dd, J = 3.6 Hz, 52.0 Hz, 1H), 5.98 (m, 1H), 6.26 (dd, J = 3.7 Hz, 21.1 Hz, 1H), 6.67–6.72 (m, 4H), 7.11–7.17 (m, 7H), 7.28–7.55 (m, 12H), 7.57 (s, 1H), 8.65 (s, 1H); ^{13}C{^{1}H} NMR (101 MHz, $CDCl_3$) δ: 12.6, 19.2, 24.8, 26.9, 28.6, 39.7, 55.3, 73.0, 83.2, 83.4, 85.8, 86.5, 95.4, 97.4, 110.3, 113.1, 127.0, 127.8, 128.07, 128.13, 128.3, 130.2, 130.36, 130.42, 132.1, 132.4, 135.7, 136.3, 136.8, 137.4, 146.0, 150.2, 158.6, 158.7, 163.6; ^{19}F NMR (376 MHz, $CDCl_3$) δ: −121.08 (d, J = 69.34 Hz); HRMS (ESI-TOF) m/z calcd for $C_{52}H_{55}F_4N_3NaO_8Si$ $[M + Na]^+$, 976.3592, found 976.3613.

(*S*)-5′-*O*-[Bis(4-methoxyphenyl)phenylmethyl]-2′-β-fluoro-5′-*C*-trifluoroacetylaminopropyl-thymidine (18)

Tetrabutylammonium fluoride (TBAF, 2.25 mL of a 1 M solution in THF) was added in a solution of compound **17** (0.997 g, 1.05 mmol) in THF (22.5 mL) under argon atmosphere, and the reactant was stirred for 2 h at room temperature. The reactant was extracted with ethyl acetate and saturated $NaHCO_3$; the organic layer was washed with brine, dried by Na_2SO_4, filtered and concentrated. The crude material was purified by column chromatography (67% ethyl acetate in hexane) to afford desired product **18** as a white solid (0.713 g, 95%). ^{1}H NMR (400 MHz, acetonitrile-d_3) δ: 1.11–1.41 (m, 4H), 1.75 (s, 3H), 2.88–2.96 (m, 2H), 3.41–3.45 (m, 1H), 3.75–3.80 (m, 7H), 4.33–4.42 (m, 1H), 4.92 (ddd, J = 2.3 Hz, 4.1 Hz, 52.7 Hz, 1H), 6.06 (dd, J = 4.1 Hz, 17.0 Hz, 1H), 6.83–6.87 (m, 4H), 7.20–7.53 (m, 9H), 7.46 (s, 1H), 9.10 (s, 1H); ^{13}C{^{1}H} NMR (101 MHz, acetonitrile-d_3) δ: 12.7, 25.2, 29.1, 40.3, 55.9, 73.7, 75.2, 75.5, 83.2, 83.4, 83.6, 87.4, 96.8, 98.7, 110.4, 113.90, 113.93, 127.8, 128.7, 129.1, 131.4, 137.4, 137.6, 137.8, 147.7, 151.1, 159.76, 159.79, 164.4; ^{19}F NMR (376 MHz, acetonitrile-d_3) δ: −120.69 (broad s); HRMS (ESI-TOF) m/z calcd for $C_{36}H_{37}F_4N_3NaO_8$ $[M + Na]^+$, 738.2415, found 738.2409.

3′-*O*-[2-Cyanoethoxy(diisopropylamino)phosphino]-(*S*)-5′-*O*-[bis(4-methoxyphenyl)phenylmethyl]-2′-β-fluoro-5′-*C*-trifluoroacetylaminopropyl-thymidine (19)

N,*N*-Diisopropylethylamine (DIPEA, 0.85 mL, 4.87 mmol) and 2-cyanoethyl *N*,*N*-diisopropylchlorophosphoramidite (CEPCl, 0.45 mL, 2.00 mmol) were added in a solution of compound **18** (0.713 g, 1.00 mmol) in THF (7.00 mL) in turn under argon atmosphere. The reactant was stirred for 1.5 h at room temperature, and then extracted with ethyl acetate and saturated $NaHCO_3$; the organic layer was washed with brine, dried by Na_2SO_4, filtered and concentrated. The crude material was purified by column chromatography (60% ethyl acetate in hexane) to afford desired product **19** as a white solid (0.813 g, 89%). ^{19}F NMR (376 MHz, $CDCl_3$) δ: −119.58 (broad s); ^{31}P NMR

(162 MHz, $CDCl_3$) δ: 152.1, 151.7; HRMS (ESI-TOF) m/z calcd for $C_{45}H_{54}F_4N_5NaO_9P$ $[M + Na]^+$, 938.3493, found 938.3500.

(*S*)-5′-*C*-Allyl-2′-β-fluoro-3′,5′-[1,1,3,3-tetraisopropyl-1,3-disiloxanediyl]-thymidine (20)

Tetrabutylammonium fluoride (TBAF, 0.39 mL of a 1 M solution in THF) was added in a solution of compound **11** (0.095 g, 0.18 mmol) in THF (3.9 mL) under argon atmosphere, and the reactant was stirred for 2 h at room temperature. The reactant was extracted with ethyl acetate and saturated $NaHCO_3$; the organic layer was washed with brine, dried by Na_2SO_4, filtered and concentrated. The residue was dissolved with pyridine (1.10 mL) and 1,3-dichloro-1,1,3,3-tetraisopropyldisiloxane ($TIPDSCl_2$, 0.11 mL, 0.34 mmol) was added at 0 °C. The reactant was stirred for 24 h at room temperature and then extracted with chloroform and saturated $NaHCO_3$; the organic layer was washed with brine, dried by Na_2SO_4, filtered and concentrated. The crude material was purified by column chromatography (100% chloroform) to afford desired product **20** as a white solid (0.082 g, 83%). ^{1}H NMR (400 MHz, $CDCl_3$) δ: 0.96–1.12 (m, 28H), 1.92 (d, J = 0.92 Hz, 3H), 2.38–2.56 (m, 2H), 3.61–3.69 (m, 1H), 4.05 (m, 1H), 4.45 (m, 1H), 5.07–5.24 (m, 3H), 5.75–5.85 (m, 1H), 6.23 (dd, J = 6.0 Hz), 7.27 (s, 1H), 8.92 (s, 1H); ^{13}C{^{1}H} NMR (101 MHz, $CDCl_3$) δ: 12.5, 12.7, 12.8, 13.2, 13.6, 16.9, 17.0, 17.1, 17.49, 17.53, 37.4, 68.6, 73.3, 73.5, 79.7, 79.8, 81.0, 81.2, 93.5, 95.5, 110.8, 118.5, 133.7, 135.9, 150.4, 163.7; ^{19}F NMR (376 MHz, $CDCl_3$) δ: −120.62 (d, J = 92.42 Hz); HRMS (ESI-TOF) m/z calcd for $C_{25}H_{43}FN_2NaO_6Si_2$ $[M + Na]^+$, 565.2541, found 565.2532.

(*R*)-5′-*C*-Allyl-2′-β-fluoro-3′,5′-[1,1,3,3-tetraisopropyl-1,3-disiloxanediyl]-thymidine (21)

Tetrabutylammonium fluoride (TBAF, 0.80 mL of a 1 M solution in THF) was added in a solution of compound **12** (0.1817 g, 0.34 mmol) in THF (7.3 mL) under argon atmosphere, and the reactant was stirred for 2 h at room temperature. The reactant was extracted with ethyl acetate and saturated $NaHCO_3$; the organic layer was washed with brine, dried by Na_2SO_4, filtered and concentrated. The half of residue was dissolved with pyridine (1.00 mL) and 1,3-dichloro-1,1,3,3-tetraisopropyldisiloxane ($TIPDSCl_2$, 0.11 mL, 0.34 mmol) was added at 0 °C. The reactant was stirred for 24 h at room temperature and then extracted with chloroform and saturated $NaHCO_3$; the organic layer was washed with brine, dried by Na_2SO_4, filtered and concentrated. The crude material was purified by column chromatography (100% chloroform) to afford desired product **21** as a white solid (0.067 g, 87%). ^{1}H NMR (400 MHz, $CDCl_3$) δ: 0.90–1.26 (m, 28H), 1.95 (d, J = 0.92 Hz, 3H), 2.27–2.34 (m, 1H), 2.50–2.55 (m, 1H), 3.51 (dd, J = 5.3 Hz, 9.2 Hz, 1H), 4.00–4.05 (m, 1H), 4.41 (dd, J = 5.3 Hz, 26.4 Hz, 1H), 4.98–5.16 (m, 3H), 5.88–5.99 (m, 1H), 6.05 (dd, J = 3.2 Hz, 21.1 Hz, 1H), 7.21 (dd, J = 1.4 Hz, 2.3 Hz, 1H), 8.74 (s, 1H); ^{13}C{^{1}H} NMR (101 MHz, $CDCl_3$) δ: 12.7, 13.2, 13.3, 13.6, 16.9, 17.1, 17.6, 17.8, 17.9, 39.7, 74.8, 79.6, 79.9, 85.1, 110.4, 118.1, 134.0, 136.7, 150.2, 163.5; ^{19}F NMR (376 MHz, $CDCl_3$) δ: −117.58 (q, J = 23.11 Hz, 46.23 Hz); HRMS (ESI-TOF) m/z calcd for $C_{25}H_{43}FN_2NaO_8Si_2$ $[M + Na]^+$, 565.2541, found 565.2554.

Solid-phase oligonucleotide synthesis

The synthesis was carried out with a DNA/RNA synthesizer by the phosphoramidite method. After the synthesis, the RNA oligomers were cleaved from CPG beads and deprotected by treatment with concentrated NH_3 solution/40% methylamine (1 : 1, v/v) for 10 min at 65 °C, while the DNA oligomers were treated with concentrated NH_3 solution for 12 h at 55 °C. Notably, before the treatment of the NH_3 solution, the CPG beads were treated with 10% dimethylamine in MeCN for 5 min followed by a rinse with MeCN to selectively remove cyanoethyl groups, if there are analogs introduced in oligomers. Then, 2′-*O*-TBDMS groups in RNA oligomers were removed by $Et_3N{\cdot}3HF$ (125 μL) in DMSO (100 μL) for 1.5 h at 65 °C. The reaction was quenched with 0.1 M TEAA buffer (pH 7.0) and the mixture was desalted using a Sep-Pak C18 cartridge. The oligomers were purified by 20% PAGE containing 7 M urea to give highly purified oligonucleotides.

MALDI-TOF/MS analysis of ONs

The spectra were obtained with a time-of-flight mass spectrometer equipped with a nitrogen laser (337 nm, 3 ns pulse). A solution of 3-hydroxypicolinic acid (3-HPA) and diammonium hydrogen citrate in H_2O was used as a matrix. Data of synthetic ONs: DNA **1**: m/z = 4712.78 (calcd for $C_{154}H_{203}N_{38}O_{104}P_{15}$ $[M - H]^-$, 4713.60); DNA **2**: m/z = 4941.01 (calcd for $C_{166}H_{231}N_{42}O_{104}P_{15}$ $[M - H]^-$, 4943.23); DNA **3**: m/z = 5012.98 (calcd for $C_{166}H_{227}F_4N_{42}O_{104}P_{15}$ $[M - H]^-$, 5014.16); DNA **5**: m/z = 4044.76 (calcd for $C_{131}H_{168}N_{50}O_{77}P_{12}$ $[M - H]^-$, 4043.31); DNA **6**: m/z = 4062.75 (calcd for $C_{131}H_{167}FN_{50}O_{77}P_{12}$ $[M - H]^-$, 4061.76); DNA **7**: m/z = 5250.91 (calcd for $C_{181}H_{228}N_{39}O_{113}P_{16}$ $[M - H]^-$, 5252.09); DNA **8**: m/z = 5479.15 (calcd for $C_{193}H_{256}N_{43}O_{113}P_{16}$ $[M - H]^-$, 5481.17); DNA **9**: m/z = 5551.11 (calcd for $C_{193}H_{252}F_4N_{43}O_{113}P_{16}$ $[M - H]^-$, 5552.23); DNA **10**: m/z = 4787.83 (calcd for $C_{157}H_{209}FN_{39}O_{104}P_{15}$ $[M - H]^-$, 4789.59); DNA **11**: m/z = 4787.83 (calcd for $C_{157}H_{209}FN_{39}O_{104}P_{15}$ $[M - H]^-$, 4790.08); DNA **12**: m/z = 4787.83 (calcd for $C_{157}H_{209}FN_{39}O_{104}P_{15}$ $[M - H]^-$, 4789.44); DNA **13**: m/z = 4787.83 (calcd for $C_{157}H_{209}FN_{39}O_{104}P_{15}$ $[M - H]^-$, 4790.53); RNA **1**: m/z = 5298.85 (calcd for $C_{160}H_{193}N_{80}O_{100}P_{15}$ $[M - H]^-$, 5300.40); RNA **6**: m/z = 5836.99 (calcd for $C_{187}H_{218}N_{81}O_{109}P_{16}$ $[M - H]^-$, 5838.61). The other ONs, which have been used in this study but not mentioned above, were synthesized in the previous study.[14]

Reverse-phase HPLC analysis of ONs

The purity of each synthesized ONs in this study was evaluated by reverse-phase HPLC (C18G 5 μm, 150 × 4.6 mm SS). Elution started from 100% buffer A, followed by a linear gradient to 35% buffer B in 20 min at a flow rate of 1.0 mL min^{-1} (buffer A: 5% MeCN in 0.1 M TEAA (pH 7.0); buffer B: 50% MeCN in 0.1 M TEAA (pH 7.0).)

Thermal denaturation study

The solution containing 3.0 μM DNA/RNA duplex in a buffer of 10 mM sodium phosphate (pH 7.0) containing 100 mM NaCl was heated at 90–100 °C and then cooled gradually to room

temperature, and used for the thermal denaturation study. Thermally induced transitions were monitored at 260 nm with a UV/vis spectrometer fitted with a temperature controller in quartz cuvettes with a path length of 1.0 cm. The sample temperature was increased by 0.5 °C min^{-1}. The thermodynamic parameters of the duplexes on duplex formation were determined by calculations based on the slope of a $1/T_m$ *vs.* $\ln(C_T/4)$ plot, where C_T (1, 3, 6, 12, 15, 21, 30 and 60 μM) is the total concentration of single strands.

CD spectroscopy

All CD spectra were recorded at 25 °C. The following instrument settings were used: resolution, 1 nm; response 1.0 s; speed, 50 nm min^{-1}; accumulation, 10.

Molecular modeling study

The initial geometry of the natural thymidine, (*S*)-5′-*C*-aminopropyl-thymidine and (*S*)-5′-*C*-aminopropyl-2′-β-fluoro-thymidine were modeled by a molecular modeling software, SYBYL.[25] The geometry of each nucleoside was optimized and the electrostatic potential (ESP) of each nucleoside was calculated by Gaussain16 at the HF/6-31G* level of theory.[26] The restrained ESP (RESP) charges were derived using the Antechamber RESP fitting procedure.[27] The generalized AMBER force field (GAFF) was used to natural and modified nucleosides.[28] Each of the nucleoside was solvated in a cubic box with TIP3P water model and periodic boundary conditions were applied.[29] The size of cubic box was determined to be 43.0 Å lengths based on the molecular size of (*S*)-5′-*C*-aminopropyl-2′-β-fluoro-thymidine. Chloride ions were added into the solution to neutralize the charge of the systems. The energy minimization calculation was performed using the SANDER module of AMBER18. The calculation of the solute molecule was carried out by 2500 circles of the steepest descent method followed by 2500 circles of the conjugate gradient method, applying a restraint force constant of 2.0 kcal (mol $Å^2$) $^{-1}$ to the nucleoside. Then, the calculation of the entire system was carried out by 5000 circles of the conjugate gradient method without any restraints. After that, the temperature of the system was heated gradually from 0 K to 300 K over a period of 100 ps of *NVT* dynamics with a restraint force constant of 2.0 kcal (mol $Å^2$) $^{-1}$ to the nucleoside, followed by 50 ps of *NPT* equilibration at 300 K and 1 bar pressure with the same restraint force. After the equilibration phase, 500 ns MD simulations were performed in an *NPT* ensemble at 300 K and 1 bar pressure without any restraints. During all MD simulations, a time step of 2 fs was used. The cutoff distance towards the van der Waals force was 10 Å, the SHAKE algorithm was used to constrain all bonds involving hydrogen atoms, and the Particle Mesh Ewald (PME) method was used for long-range electrostatic interaction.[30,31] The temperature was regulated by Langevin dynamics with a collision frequency of 2.0 ps^{-1}.[32] All the MD simulations were performed by the PMEMD module of AMBER18.[33] Trajectory analysis was done for 50 000 snapshots, every 10 ps, sampled during the full 500 ns simulation.

Nuclease resistance of single-stranded DNA

Fluorescein labeled DNAs (300 pmol) were dissolved in OPTI-MEM (37.5 μL) and used for the serum stability test. 1.2 μL bovine serum was added, and subsequently the mixture was incubated at 37 °C for the required time. Aliquots of 2.4 μL were diluted with a stop solution (10 mM EDTA in formamide 10 μL). Samples were subjected to electrophoresis in 20% PAGE containing 7 M urea and quantified by Luminescent Image analyzer LAS-4000 (Fujifilm).

RNase H assay

The DNA/RNA duplexes used for RNase H assay were prepared by mixing the DNAs (600 pmol) with fluorescein labeled complementary target RNA (3000 pmol) in 75 μL of 50 mM Tris–HCl (pH 8.0) containing 75 mM KCl, 3 mM $MgCl_2$ and 10 mM dithiothreitol, followed by heating at 90–100 °C for 5 min and cooling gradually to room temperature. Then, 70 μL diluted RNase H solution (60 unit per L in H_2O) was added, and subsequently the mixture was incubated at 37 °C for the required time. Aliquots of 5 μL were diluted with 100% formamide (10 μL). Samples were subjected to electrophoresis in 20% PAGE containing 7 M urea and quantified by Luminescent Image analyzer LAS-4000 (Fujifilm).

Conflicts of interest

There are no conflicts to declare.

Acknowledgements

This work was supported by the Japan Agency for Medical Research and Development (AMED) through its Funding Program for Basic Science and Platform Technology Program for Innovative Biological Medicine, development of siRNA conjugates with tissue-specific delivery functions (18am0301022h0004).

References

1 K. E. Lundin, O. Gissberg and C. I. Smith, Oligonucleotide therapies: the past and the present, *Hum. Gene Ther.*, 2015, **26**, 475–485.
2 D. A. Bell, A. J. Hooper and J. R. Burnett, Mipomersen, an antisense apolipoprotein B synthesis inhibitor, *Expert Opin. Invest. Drugs*, 2011, **20**, 265–272.
3 T. Gidaro and L. Servais, Nusinersen treatment of spinal muscular atrophy: current knowledge and existing gaps, *Dev. Med. Child Neurol.*, 2019, **61**, 19–24.
4 M. D. Benson, M. Waddington-Cruz, J. L. Berk, M. Polydefkis, *et al.*, Inotersen Treatment for Patients with Hereditary Transthyretin Amyloidosis, *N. Engl. J. Med.*, 2018, **379**, 22–31.
5 J. Paik and S. Duggan, Volanesorsen: first global approval, *Drugs*, 2019, **79**, 1349–1354.
6 R. R. Roshmi and T. Yokota, Viltolarsen for the treatment of Duchenne muscular dystrophy, *Drugs Today*, 2019, **55**, 627–639.

7 (*a*) M. Manoharan, Oligonucleotide Conjugates as Potential Antisense Drugs with Improved Uptake, Biodistribution, Targeted Delivery, and Mechanism of Action, *Antisense Nucleic Acid Drug Dev.*, 2002, **12**, 103–128; (*b*) T. Aboul-Fadl, Antisense Oligonucleotides: The State of the Art, *Curr. Med. Chem.*, 2005, **12**, 2193–2214; (*c*) S. T. Crooke, Molecular Mechanisms of Antisense Oligonucleotides, *Nucleic Acid Ther.*, 2017, **27**, 70–77.

8 S. T. Crooke, S. Wang, T. A. Vickers, W. Shen and X.-h. Liang, Cellular uptake and trafficking of antisense oligonucleotides, *Nat. Biotechnol.*, 2017, **35**, 230–237.

9 W. Shen, C. L. De Hoyos, H. Sun, T. A. Vickers, X.-h. Liang and S. T. Crooke, Acute hepatotoxicity of 2′-fluoro-modified 5–10–5 gapmer phosphorothioate oligonucleotides in mice correlates with intracellular protein binding and the loss of DBHS proteins, *Nucleic Acids Res.*, 2018, **46**, 2204–2217.

10 W. Shen, C. L. De Hoyos, M. T. Migawa, T. A. Vickers, *et al.*, Chemical modification of PS-ASO therapeutics reduces cellular protein-binding and improves the therapeutic index, *Nat. Biotechnol.*, 2019, **37**, 640–650.

11 M. Kanazaki, Y. Ueno, S. Shuto and A. Matsuda, Highly Nuclease-Resistant Phosphodiester-Type Oligodeoxynucleotides Containing 4′-α-*C*-Aminoalkylthymidines Form Thermally Stable Duplexes with DNA and RNA. A Candidate for Potent Antisense Molecules, *J. Am. Chem. Soc.*, 2000, **122**, 2422–2432.

12 K. Koizumi, Y. Maeda, T. Kano, *et al.*, Synthesis of 4′-*C*-aminoalkyl-2′-*O*-methyl modified RNA and their biological properties, *Bioorg. Med. Chem.*, 2018, **26**, 3521–3534.

13 T. Kano, Y. Katsuragi, Y. Maeda and Y. Ueno, Synthesis of 4′-*C*-aminoalkyl-2′-*O*-methyl modified RNA and their biological properties, *Bioorg. Med. Chem.*, 2018, **26**, 4574–4582.

14 T. Tsuchihira, R. Kajino, Y. Maeda and Y. Ueno, 4′-*C*-Aminomethyl-2′-deoxy-2′-fluoroarabinonucleoside increases the nuclease resistance of DNA without inhibiting the ability of a DNA/RNA duplex to activate RNase H, *Bioorg. Med. Chem.*, 2020, **28**, 115611.

15 R. Kajino, Y. Maeda, H. Yoshida, K. Yamagishi and Y. Ueno, Synthesis and biophysical characterization of RNAs containing (*R*)- and (*S*)-5′-C-aminopropyl-2′-*O*-methyluridines, *J. Org. Chem.*, 2019, **84**, 3388–3404.

16 H. Inoue, Y. Hayase, S. Iwai and E. Ohtsuka, Sequence-dependent hydrolysis of RNA using modified oligonucleotide splints and RNase H, *FEBS Lett.*, 1987, **215**, 327–330.

17 A. T. Daniher, J. Xie, S. Mathur and J. K. Bashkin, Modulation of RNase H activity by modified DNA probes: major groove vs. minor groove effects, *Bioorg. Med. Chem.*, 1997, **5**, 1037–1042.

18 C. J. Wilds and M. J. Damha, 2′-Deoxy-2′-fluoro-β-D-arabinonucleosides and oligonucleotides (2′-F-ANA): synthesis and physicochemical studies, *Nucleic Acids Res.*, 2000, **28**, 3625–3635.

19 M. J. Damha, C. J. Wilds, A. Noronha, *et al.*, Hybrids of RNA and Arabinonucleic Acids (ANA and 2′-F-ANA) Are Substrates of Ribonuclease H, *J. Am. Chem. Soc.*, 1998, **120**, 12976–12977.

20 J. K. Watts, N. Martín-Pintado, I. Gómez-Pinto, *et al.*, Differential stability of 2′-F-ANA·RNA and ANA·RNA hybrid duplexes: roles of structure, pseudohydrogen bonding, hydration, ion uptake and flexibility, *Nucleic Acids Res.*, 2010, **38**, 2498–2511.

21 P. Magdalena, P. Ondřej, B. Miloš, *et al.*, Straightforward synthesis of purine 4′-alkoxy-2′-deoxynucleosides: first report of mixed purine–pyrimidine 4′-alkoxyoligodeoxynucleotides as new RNA mimics, *Org. Lett.*, 2015, **17**, 3426–3429.

22 B. Valerie and E. Jean-Marc, Allylsilanes in the preparation of 5′-*C*-hydroxy or bromo alkylthymidines, *Tetrahedron*, 1999, **55**, 5831–5838.

23 S. Shahien, C. Jinsen, W. Travis, *et al.*, Tritylation of alcohols under mild conditions without using silver salts, *Tetrahedron Lett.*, 2016, **57**, 3877–3880.

24 R. G. Parmar, C. R. Brown, S. Matsuda, *et al.*, Facile synthesis, geometry, and 2′-substituent-dependent in vivo activity of 5′-(*E*)- and 5′-(*Z*)-vinylphosphonate-modified siRNA conjugates, *J. Med. Chem.*, 2018, **61**, 734–744.

25 *SYBYL-X Suite*, version 2.1.1, Certara, Princeton, NJ, 2012.

26 J. F. Michael, W. T. Gary and H. S. Bernhard, *et al.*, Gaussian, Inc., Wallingford CT, 2016.

27 I. B. Christopher, C. Piotr, C. Wendy and A. K. Peter, A well-behaved electrostatic potential based method using charge restraints for deriving atomic charges: the RESP model, *J. Phys. Chem.*, 1993, **97**, 10269–10280.

28 W. Junmei, M. W. Romain, W. C. James, A. K. Peter and A. C. David, Development and testing of a general amber force field, *J. Comput. Chem.*, 2004, **25**, 1157–1174.

29 L. J. William, C. Jayaraman and D. M. Jeffry, Comparison of simple potential functions for simulating liquid water, *J. Chem. Phys.*, 1983, **79**, 926–935.

30 P. R. Jean, C. Giovanni and J. C. B. Herman, Numerical integration of the cartesian equations of motion of a system with constraints: molecular dynamics of *n*-alkanes, *J. Comput. Phys.*, 1977, **23**, 327–341.

31 D. Tom, Y. Darrin and P. Lee, Particle mesh Ewald: an $N\log(N)$ method for Ewald sums in large systems, *J. Chem. Phys.*, 1993, **98**, 10089–10092.

32 W. P. Richard, R. B. Bernard and S. Attila, An analysis of the accuracy of Langevin and molecular dynamics algorithms, *Mol. Phys.*, 1988, **65**, 1409–1419.

33 A. C. David, Y. B. Ido and R. B. Scott, *et al.*, *AMBER 2018*, University of California, San Francisco, 2018.

